A Novel Vehicle Detection Method With High Resolution Highway Aerial Image

Zezhong Zheng, *Member, IEEE*, Guoqing Zhou, *Senior Member, IEEE*, Yong Wang, Yalan Liu, Xiaowen Li, Xiaoting Wang, and Ling Jiang, *Member, IEEE*

***Abstract*—A robust and efficient vehicle detection method from high resolution aerial image is still challenging. In this paper, a novel and robust method for automatic vehicle detection using aerial images over highway was presented. In the method, a GIS road vector map was used to constrain the vehicle detection system to the highway networks. After the morphological structure element was identified, we utilized the grayscale opening transformation and grayscale top-hat transformation to identify hypothesis vehicles in the light or white background, and used the grayscale closing transformation and grayscale bot-hat transformation to identify the hypothesis vehicles in the black or dark background. Then, targets with large size or covering a large area were sieved from the hypothesis vehicles using an area threshold that is much larger than a typical vehicle. Targets, whose width is narrower than the diameter of structure element utilized in the grayscale morphological transformation, were smoothed out from the hypothesis vehicles using binary morphological opening transformation. Finally, the hypothesis vehicles detected in both cases were overlaid. It should be noted that in the detection system, a vehicle could be detected twice by the two approaches. The two identical hypothesis vehicles should be amalgamated into a single one for accuracy assessment subsequently. We tested our system on seventeen highway scenes of aerial images with a spatial resolution of 0.15 × 0.15 m. The experimental results showed that the correctness, completeness, and quality rates of the proposed vehicle detection method were about 98%, 93%, and 92%, respectively. Thus, our proposed approach is robust and efficient to detect vehicles of highway using high resolution aerial images.**

***Index Terms*—Grayscale bot-hat transformation, grayscale top-hat transformation, structure element, vehicle detection.**

Manuscript received February 07, 2013; revised April 11, 2013; accepted May 30, 2013. Date of publication June 25, 2013; date of current version November 21, 2013. The work was supported in part by Open Fund of State Key Laboratory of Remote Sensing Science (Grant No. OFSLRSS201318); National Natural Science Foundation of China (Grant No. 91024004, Grant No. 41162011, and Grant No. 41201388); Fundamental Research Funds for the Central Universities, China (Grant No. ZYGX2011J081); Opening Foundation of Guangxi Key Laboratory for Spatial Information and Geomatics, Guangxi, China (Grant No. GKN1103108-19 and Grant No. GKN1207115-16); and Special Fund for Special Public Welfare Ministry of Environmental Protection, China (Grant No. 201009063). *(Corresponding author: G. Zhou.)*

Z. Zheng is with the School of Resources and Environment, University of Electronic Science and Technology of China (UESTC), Chengdu, Sichuan 611731, China, and with State Key Laboratory of Remote Sensing Science, Jointly Sponsored by Beijing Normal University and the Institute of Remote Sensing and Digital Earth of Chinese Academy of Sciences, Beijing 100101, China, and also with Guangxi Key Laboratory for Spatial Information and Geomatics, Guilin University of Technology, Guilin, Guangxi 541004, China (e-mail: zezhongzheng @uestc.edu.cn).

G. Zhou is with Guangxi Key Laboratory for Spatial Information and Geomatics, Guilin University of Technology, Guilin, Guangxi 541004, China (e-mail: zgq@glite.edu.cn).

Y. Wang is with the School of Resources and Environment, University of Electronic Science and Technology of China (UESTC), Chengdu, Sichuan 611731, China, and also with the Department of Geography, East Carolina University, Greenville, NC 27858 USA (e-mail: wangy2012@uestc.edu.cn).

Y. Liu is with the Institute of Remote Sensing and Digital Earth, Chinese Academy of Sciences, Beijing 100094, China (e-mail: liuyl@irsa.ac.cn).

X. Li is with the State Key Laboratory of Remote Sensing Science, Jointly Sponsored by Beijing Normal University and the Institute of Remote Sensing and Digital Earth of Chinese Academy of Sciences, Beijing 100101, China (e-mail: lix@bnu.edu.cn).

X. Wang is with the School of Resource and Environment, Chengdu University of Information Technology, Chengdu, Sichuan 610225, China (e-mail: wangxting@126.com).

L. Jiang is with the School of Resources and Environment, University of Electronic Science and Technology of China (UESTC), Chengdu, Sichuan 611731, China (e-mail: jiangl_sre@uestc.edu.cn).

Color versions of one or more of the figures in this paper are available online at http://ieeexplore.ieee.org.

Digital Object Identifier 10.1109/JSTARS.2013.2266131

I. Introduction

With rapid increase of traffic volume and constant road congestion, there is a high demand for traffic monitoring, especially in urban areas. Currently, monitoring and mitigation are implemented using a lot of ground sensors such as induction loop detectors [1]–[3], bridge sensors and stationary cameras [4]–[7]. However, these sensors can only partially acquire the traffic information of major arterials in urban areas. The traffic conditions of the majority of highways are seldom collected [2], [8], [9]. Hence, area-wide images of the entire highway networks are required to complement the traffic conditions that are ground-based and selective. Vehicles, even small cars, can be clearly identified on high resolution aerial images with a ground resolution of 0.15 × 0.15 m. Thus, using the high resolution aerial imagery to detect vehicles for traffic monitoring and mitigation of an area with a large spatial extent is very attractive.

Of existing vehicle detection methods using aerial imagery [10]–[15], two types of vehicle models have been basically used: 1) an appearance-based implicit model, and 2) an explicit model. The implicit model typically consists of image intensity or texture features computed using a small window or kernel that surrounds a given pixel or a small clusters of pixels. Detection is conducted by examining feature vectors of the immediate surrounding pixels of the image. For example, Ruskone *et al.* [10] utilized aerial imagery with 0.3–0.4 m resolutions to develop a two-step analysis strategy that is composed of vehicle detection, and then validation through line clustering. In the detection, the intensity values of surrounding pixels were analyzed using a multilayer perceptron (MLP). For the validation, the perceptual grouping theory was used to group the vehicles into lines. In addition, Papageorgiou and Poggio [13] presented a trainable system for the vehicle detection from aerial imagery taken from a stationary camera. A Haar wavelet

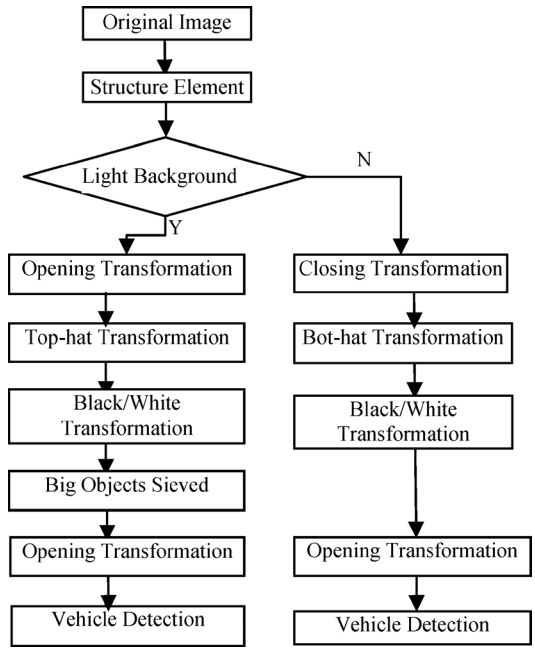

Fig. 1. Flowchart of the proposed vehicle detection method.

transformation was employed to describe the object classes in terms of local, directional, and multi-scale differences of intensity around adjacent regions. The detection model was derived through the training of a support vector machine classifier using numerous positive and negative examples of vehicles. Of the explicit models, a vehicle is usually described by a box or wire-frame representation. Detection is carried out by matching the model to the image with a "top-down" strategy, or grouping low-level features to construct structures similar to the model using a "bottom-up" approach. For instance, a vehicle has been represented as a 3-D box with dimensions in width, length and height [14], [15]. Site models were used to constrain vehicles in parking lots or on roads.

Of these early efforts or studies, the approaches are time consuming, although some methods offer promising results [4]–[7], it is still questionable whether or not they are operational [10], [16]–[18]. In addition, the overall accuracy in vehicle detection can be low or unsatisfactory [1], [3], [6]. In our study, we present a method to detect vehicles in light or white background with grayscale opening transformation and grayscale top-hat transformation, and to detect vehicles in black or dark background with grayscale closing transformation and grayscale bot-hat transformation, respectively.

II. Methods

The proposed method includes the following major steps. First, the structure element of morphological transformation is identified. Then, the grayscale opening transformation, grayscale top-hat transformation, and Otsu partitioning method are employed to detect vehicles in light background. Whereas the grayscale closing transformation, grayscale bot-hat transformation, and Otsu partitioning method are utilized to detect vehicles in black background. The flowchart of our proposed method is shown in Fig. 1.

Fig. 2. A highway image with a spatial resolution of 0.15 × 0.15 m.

A. Structure Element Identification

A vehicle's length varies from a couple of meters for a car to tens of meters for a car with a long trailer or a semi-truck. However, the width of a vehicle is around 2 m. On an image with a spatial resolution of 0.15 × 0.15 m (Fig. 2), the number of pixels in width dimension is 13–14 pixels. Because the vehicle in width dimension (e.g., a car) tends to be symmetrical, a disc with a radius of about 5 pixels is our structure element. Its diameter is a little smaller than the width of the vehicle.

B. Gray-Scale Morphological Method

Because the detailed discussions of grayscale morphological method can be found in [19]–[22], the grayscale opening transformation and grayscale closing transformation are directly presented here as

$$\text{Opening}: f \circ b = (f \Theta b) \oplus b \tag{1}$$

$$\text{Closing}: f \bullet b = (f \oplus b) \Theta b \tag{2}$$

where f presents the original highway image, b is the structure element, $\circ$ presents the grayscale opening transformation, and $\bullet$ presents the grayscale closing transformation. Θ and $\oplus$ are an erosion operator and a dilation operator, respectively. The grayscale top-hat transformation and grayscale bot-hat transformation are defined as

$$\text{Top-hat}: T = f - f \circ b \tag{3}$$

$$\text{Bot-hat}: B = f \bullet b - f \tag{4}$$

where T presents the image after the grayscale top-hat transformation, and B is the image after the grayscale bot-hat transformation.

C. Background Estimation

On the one hand, after the grayscale opening transformation, bright pixels representing dashed white lines for lane division and concrete road dividers with bright surface background, as well as a little target of bright color can be filtered out as noise. Thus, the grayscale opening transformed image can be considered as an estimation of the background (Fig. 3). Then, the top-hat transformed image (Fig. 4) is derived with the original image (Fig. 2) minus the grayscale opening transformed image.

On the other hand, after the grayscale closing transformation, pixels with low intensity or small digital number (DN) can be

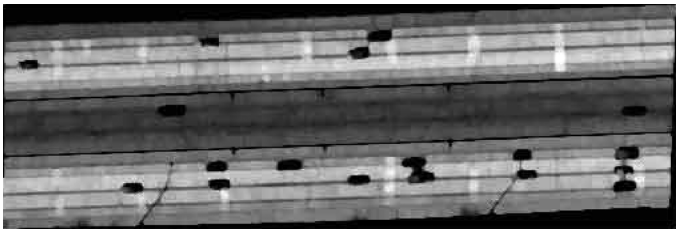

Fig. 3. A grayscale opening transformed image.

Fig. 4. A grayscale top-hat transformed image.

Fig. 5. A grayscale closing transformed image.

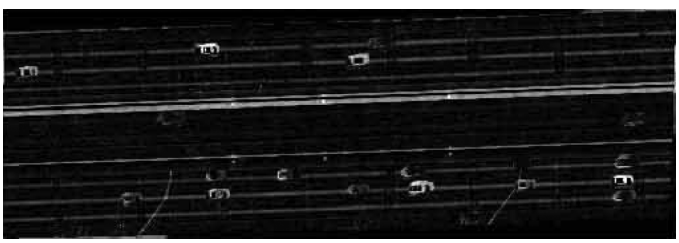

Fig. 6. A grayscale bot-hat transformed image.

filtered out as noise. The pixels could be new pavement with tar or a target with a dark or black color. Thus, the image after the grayscale closing transformation can also be considered as a background estimation as well (Fig. 5). The grayscale bot-hat transformed image (Fig. 6) is derived with the grayscale closing transformed image (Fig. 5) minus the original image (Fig. 2).

D. Vehicle Detection

The grayscale top-hat transformed image (Fig. 4) can be converted into a black and white or binary image (Fig. 7) with Otsu threshold method [23]. Since most family cars are 5 (length, m) $\times$ 2 (width, m) or less in size, the number of pixels representing a family car is around 34 $\times$ 14 pixels (for an image with a spatial resolution of 0.15 $\times$ 0.15 m). To include a car with a long trailer or a semi-truck in the vehicle detection, we set the area threshold as 2000 pixels. (As an example, a large corresponding vehicle could be 15 m or around 100 pixels long, and 3 m or around 20 pixels wide.) Then, a target with an area larger than 2000 pixels is sieved in the detection. In addition, a little target whose width is less than 10 pixels can be filtered out using the morphological opening transformation with the initial structure element of a 5-pixel radius. Thus, the vehicles in light background are detected.

Fig. 7. A grayscale top-hat transformed image after the partitioning using the Otsu's method.

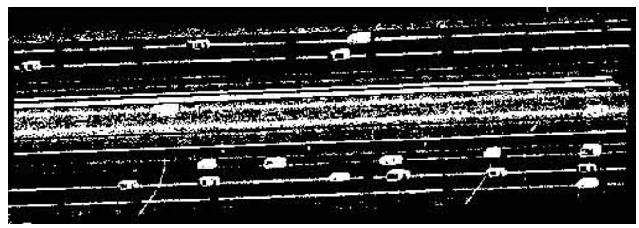

Fig. 8. A grayscale bot-hat transformed image after the partitioning using the Otsu's method.

The grayscale bot-hat transformed image (Fig. 6) can also be converted into a black and white or binary image (Fig. 8). Because the vehicle targets adhere to background together (Fig. 8), we could not sieve the false big area targets using area threshold. Otherwise, the vehicles of dark background will be sieved together with the background. However, using morphological opening transformation, we could smooth out all the little targets and other false targets, whose width is less than 10 pixels, even though their area could be very big. Thus, the vehicles of dark background and some vehicles in light background are detected.

III. Experiments and Discussion

A. Datasets

The study area was the city of Norfolk, Virginia, USA. The GIS road vector map covering streets and highways of the city was downloaded from the Hampton Roads Transportation Planning Organization (http://hrtpo.org/). The nadir-view aerial images were acquired at the same time of day in spring of 2007. The space resolution on the image was 0.15 $\times$ 0.15 m. Seventeen highway scenes were selected. (Fig. 2 was numbered as scene 3.) With a few exceptions, such as a car with a long trailer or a semi-truck, most vehicles' size is approximately 5 $\times$ 2 m or about 34 pixels in length and 14 pixels in width (e.g., Fig. 2).

B. Vehicle Extraction Results

As the method describes in Section II, from Scene 3 (Fig. 2), vehicles were detected from light background and dark background, respectively(Figs. 9 – 12). Then, the hypothesis vehi-

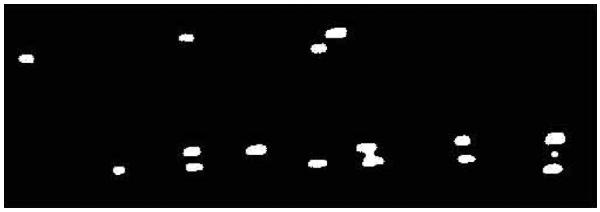

Fig. 9. Vehicle detection results using grayscale top-hat transformation.

Fig. 10. Vehicle detection results in light background.

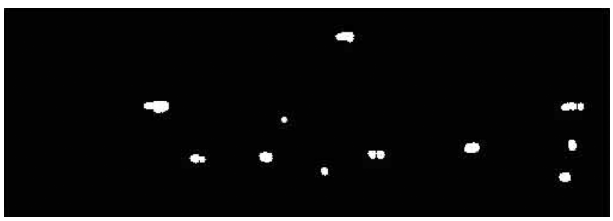

Fig. 11. Vehicle detection results using grayscale bot-hat transformation.

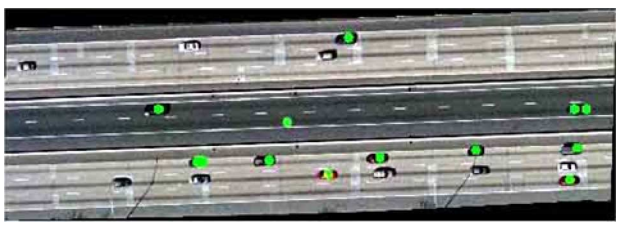

Fig. 12. Vehicle detection results in dark background.

cles detected from the two cases were overlaid (Fig. 13). The red dots (hypothesis vehicles) were detected using grayscale opening transformation and grayscale top-hat transformation, while the green dots (hypothesis vehicles) were detected using grayscale closing transformation and grayscale bot-hat transformation. The yellow dots (hypothesis vehicles) were detected twice by the two cases, and the two identical hypothesis vehicles were amalgamated to a single one with closing transformation for accuracy assessment subsequently. Fig. 14 showed the final vehicle detection results of Scene 3 with green dots. Similarly, the hypothesis vehicles of the other sixteen highway scenes were detected with the same method, and the vehicle detection results of five typical scenes were shown in Fig. 15.

In order to evaluate the vehicle detection results, a numerical accuracy assessment was conducted by comparing the number of vehicles identified manually and automatically by the proposed method. According to Wiedemann *et al.* [24], three categories of extraction results are defined as follows [5], [24], [25].

True Positive (TP): the number of correctly extracted true vehicles.

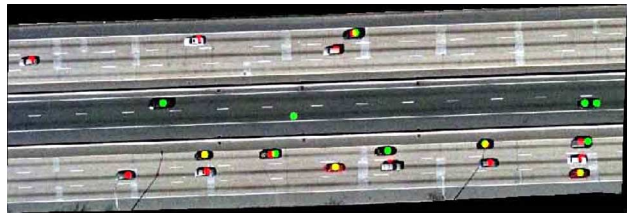

Fig. 13. Overlay of vehicle detection results from two cases.

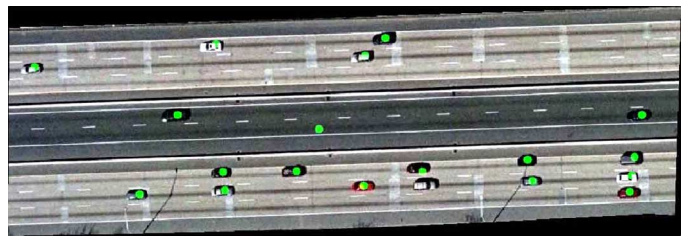

Fig. 14. Vehicle detection results from two cases.

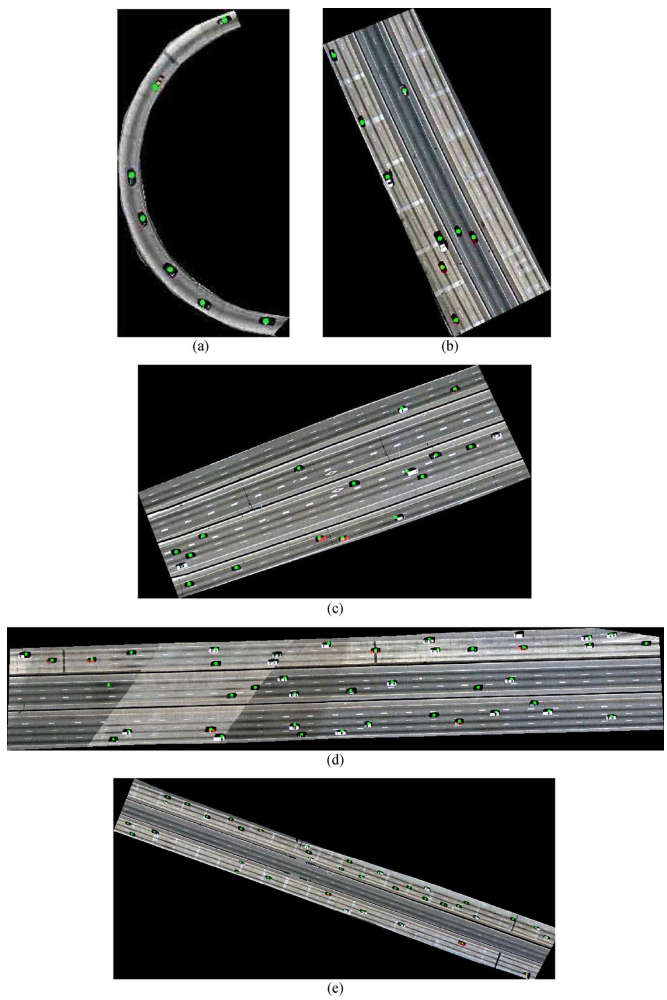

Fig. 15. Vehicle detection results of other five typical scenes. (a) Scene 1. (b) Scene 2. (c) Scene 6. (d) Scene 8. (e) Scene 12.

False Positive (FP): the number of incorrectly extracted false vehicles.

False Negative (FN): the number of omitted vehicles.

TABLE I
VEHICLE DETECTION RESULTS OF THE SEVENTEEN HIGHWAY SCENES

Highway	TP	FP	FN	Correctness(%)	Completeness(%)	Quality(%)
Scene 1	7	0	0	100.00	100.00	100.00
Scene 2	9	0	0	100.00	100.00	100.00
Scene 3	17	1	1	94.44	94.44	89.47
Scene 4	7	1	0	87.50	100.00	87.50
Scene 5	9	0	2	100.00	81.82	81.82
Scene 6	17	0	1	100.00	94.44	94.44
Scene 7	11	0	2	100.00	84.62	84.62
Scene 8	39	1	2	97.50	95.12	92.86
Scene 9	26	0	3	100.00	89.66	89.66
Scene 10	24	0	2	100.00	92.31	92.31
Scene 11	18	0	2	100.00	90.00	90.00
Scene 12	37	0	0	100.00	100.00	100.00
Scene 13	18	0	3	100.00	85.71	85.71
Scene 14	16	1	0	94.12	100.00	94.12
Scene 15	14	0	1	100.00	93.33	93.33
Scene 16	17	0	1	100.00	94.44	94.44
Scene 17	29	1	4	96.67	87.88	85.29
Total	315	5	24	98.44	92.92	91.57

Based on these three definitions, three statistical measures are used in our study:

$$\text{Correctness} = \frac{TP}{TP+FP} \times 100\% \tag{5}$$

$$\text{Completeness} = \frac{TP}{TP+FN} \times 100\% \tag{6}$$

$$\text{Quality} = \frac{TP}{TP+FP+FN} \times 100\% \tag{7}$$

The correctness is a measure ranging between 0 and 1 that indicates the detection accuracy rate relative to ground truth. The correctness and completeness are the converse of commission and omission errors, respectively. The two measures are complementary and need to be interpreted simultaneously [25]. The quality shows the overall accuracy of the extraction method, and the quality value can never be higher than either the completeness or correctness value. Table I reports the three calculated measures for the seventeen highway scenes.

C. Discussion

From Fig. 14, seventeen vehicles were detected in scene 3. Only one vehicle was omitted, and one noisy area was incorrectly extracted as a vehicle. The omitted vehicle is near to one vehicle, with white color like the background. In fact, the omitted vehicle was detected, it can be seen from Figs. 7 and 9. But the two vehicles adhere to each other. Thus, one vehicle of light background was omitted using grayscale closing transformation and grayscale top-hat transformation (Fig. 10). From Fig. 10, no false vehicles were detected from light background. While from Fig. 12, one false vehicle was detected from dark background. Since the vehicle targets of dark background adhered to the background together (Fig. 8), the false hypothesis vehicles with big area could not be sieved using area threshold. Otherwise, the vehicles of dark background could be sieved together with the background. But using morphological opening transformation we could smooth out all the little targets and other targets, whose width is less than 10 pixels. However, one false hypothesis vehicle came. In scene 3, the correctness and completeness were up to 94.44%, respectively, and the quality came up to 89.47% (Table I).

From Table I, the correctness, completeness, and quality of Scene 1, Scene 2, and Scene 12 came up to 100%, and a car with a trailer was detected in Scene 2 (Fig. 15). In Scene 6, the correctness, completeness, and quality were up to 100%, 94.44%, and 94.44%, respectively (Table I). A vehicle was omitted because of its low contrast with the light background, and a truck was detected (Fig. 15). In Scene 8, the correctness, completeness, and quality were 97.5%, 95.12%, and 92.86%, respectively (Table I). One noisy area was incorrectly extracted as a vehicle. One vehicle near to another one was omitted, and one vehicle was omitted because of its low contrast with the light background (Fig. 15).

In summary, of the 17 highway scenes, our proposed vehicle extraction method resulted in a correctness, completeness, and quality of about 98%, 93%, and 92%, respectively. Thus, the vehicle detection results of our proposed algorithm are satisfactory.

IV. CONCLUSION AND FUTURE WORK

The grayscale morphological algorithm has been developed to detect vehicles from high resolution aerial photos of highway scenes. The major components of the algorithm included the grayscale opening transformation, grayscale top-hat transformation, grayscale closing transformation, and grayscale bot-hat transformation. The GIS road vector layer was used to constrain the detection algorithm to the highway networks. Of the 17 highway scenes studied, the correctness, completeness, and quality of our proposed method were up to 98%, 93%, and 92%, respectively. Therefore, our proposed vehicle detection method is robust and efficient to detect vehicles from large scale aerial images. Our future work includes 1) optimizing the length of the disc's radius. It is expected that the optimal length of the radius will significantly improve the system and 2) detecting the vehicles occluded by trees or bridges. Our method cannot be applicable in the complex environment, because the correctness, completeness, and quality will decrease obviously, with noise increasing. We will investigate other reliable algorithms such as the morphological shared-weight neural networks (MSNN) in such case.

REFERENCES

[1] H. Zheng and L. Li, "An artificial immune approach for vehicle detection from high resolution space imagery," *Int. J. Comput. Sci. Netw. Secur.*, vol. 7, no. 2, pp. 67–72, 2007.

[2] Z. Zheng, X. Wang, G. Zhou, and L. Jiang, "Vehicle detection based on morphology from highway aerial images," in *Proc. IEEE IGARSS*, 2012, pp. 5997–6000.

[3] S. Hinz, J. Leitloff, and U. Stilla, "Context-supported vehicle detection in optical satellite images of urban areas," in *Proc. IEEE IGARSS*, 2005, vol. 4, pp. 2937–2941.

[4] W. Liu, F. Yamazaki, and T. T. Vu, "Automated vehicle extraction and speed determination from Quickbird satellite images," *IEEE J. Sel. Topics Appl. Earth Observ. Remote Sens.*, vol. 4, no. 1, pp. 75–82, 2011.

[5] F. Yamazaki and W. Liu, "Vehicle extraction and speed detection from digital aerial images," in *Proc. IEEE IGARSS*, 2008, vol. 3, pp. 1334–1337.

[6] B. Salehi, Y. Zhang, and M. Zhong, "Automatic moving vehicles information extraction from single-pass WorldView-2 imagery," *IEEE J. Sel. Topics Appl. Earth Observ. Remote Sens.*, vol. 5, no. 1, pp. 135–145, 2012.

[7] R. K. Mishra, "Automatic moving vehicle's information extraction from one-pass worldview-2 satellite imagery," in *Int. Arch. Photogramm. Remote Sens. Spatial Inform. Sci.*, 2012, vol. XXXIX-B7, XXII ISPRS Congress, pp. 323–328.

[8] G. Liu and J. Li, "Moving target detection via airborne HRR phased array radar," *IEEE Trans. Aerosp. Electron. Syst.*, vol. 37, no. 3, pp. 914–924, 2001.

[9] M. Dubuisson and A. K. Jain, "Contour extraction of moving objects in complex outdoor scenes," *Int. J. Comput. Vis.*, vol. 14, no. 1, pp. 83–105, 1995.

[10] R. Ruskone, L. Guigues, S. Airault, and O. Jamet, "Vehicle detection on aerial images: A structural approach," in *Proc. Int. Pattern Recognition*, 1996, pp. 900–904.

[11] C. Schlosser, J. Reitberger, and S. Hinz, "Automatic car detection in high resolution urban scenes based on an adaptive 3-D-model," in *Proc. 2nd GRSS/ISPRS Joint Workshop on Data Fusion and Remote Sens. over Urban Area*, 2003, pp. 167–170.

[12] G. Sharma, C. J. Merry, P. Goel, and M. McCord, "Vehicle detection in 1-m resolution satellite and airborne imagery," *Int. J. Remote Sens.*, vol. 27, no. 4, pp. 779–797, 2006.

[13] C. Papageorgiou and T. Poggio, "A trainable system for object detection," *Int. J. Comput. Vis.*, vol. 38, no. 1, pp. 15–33, 2000.

[14] P. Burlina, R. Chellappa, C. Lin, and X. Zhang, "Context-based exploitation of aerial imagery," in *IEEE Workshop on Context-Based Vision*, 1995, pp. 38–49.

[15] H. Moon, R. Chellappa, and A. Rosenfeld, "Performance analysis of a simple vehicle detection algorithm," *Image Vis. Comput.*, vol. 20, no. 1, pp. 1–13, 2002.

[16] S. Kluckner, G. Pacher, H. Grabner, H. Bischof, and J. Bauer, "A 3-D teacher for car detection in aerial images," in *Proc. IEEE Int. Conf. Comput. Vis.*, 2007, pp. 1–8.

[17] T. Nguyen, H. Grabner, B. Gruber, and H. Bischof, "On-line boosting for car detection from aerial images," in *Proc. IEEE Int. Conf. Research, Innovation and Vision for the Future (RIVF07)*, 2007, pp. 87–95.

[18] H. Grabner, T. Nguyen, B. Gruber, and H. Bischof, "On-line boosting-based car detection from aerial images," *ISPRS J. Photogramm. Remote Sens.*, vol. 63, no. 3, pp. 382–396, 2008.

[19] X. Jin and C. H. Davis, "Vehicle detection from high-resolution satellite imagery using morphological shared-weight neural networks," *Image Vis. Comput.*, vol. 25, no. 9, pp. 1422–1431, 2007.

[20] X. Jin and C. H. Davis, "Vector-guided vehicle detection from high-resolution satellite imager," in *Proc. IEEE IGARSS*, 2004, vol. 2, pp. 1095–1098.

[21] J. Serra, *Image Analysis and Mathematical Morphology*. New York, NY, USA: Academic, 1988, vol. 2.

[22] H. Chi, C. Lu, F. Zhao, and L. D. Shen, "Vehicle detection from satellite images: Intensity, chromaticity, and lane-based method," *J. Transportation Research Board, National Research Council*, pp. 109–117, 2009.

[23] N. Otsu, "A threshold selection method from gray-level histograms," *IEEE Trans. Syst., Man Cybern.*, vol. 9, no. 1, pp. 62–66, 1979.

[24] C. Wiedemann, C. Heipke, H. Mayer, and O. Jamet, "Empirical evaluation of automatically extracted road axes," in *Empirical Evaluation Methods in Computer Vision*, K. Bowyer and P. Phillips, Eds. New York, NY, USA: IEEE Comput. Soc. Press, 1998, pp. 172–187.

[25] X. Niu, "A semi-automatic framework for highway extraction and vehicle detection based on a geometric deformable model," *ISPRS J. Photogramm. Remote Sens.*, vol. 61, no. 3–4, pp. 170–186, 2006.

Zezhong Zheng (M'12) received the M.S. degree in geomatics from Chengdu University of Technology, Chengdu, China, in 2006. He received the Ph.D. degree in geomatics from Southwest Jiaotong University, Chengdu, China, in 2010. His research interest is urban remote sensing using very high resolution optical sensors.

Guoqing Zhou (M'02) received the Ph.D. degree from the Remote Sensing and Information Engineering Department, Wuhan University, Wuhan, China, in 1995. His research interest is urban remote sensing using very high resolution optical sensors and unmanned aerial vehicle.

Yong Wang received the Ph.D. degree from the University of California in 1992. His research interest includes the application of remotely sensed data to object identification.

Yalan Liu received the Ph.D. degree from the Institute of Remote Sensing and Digital Earth, Chinese Academy of Sciences, Beijing, China, in 2004. Her research interest is remote sensing in transportation.

Xiaowen Li received the Ph.D. degree from the University of California, Santa Barbara, CA, USA, in 1985. His research interests include 3-D modeling and reconstruction from multiangular remotely sensed images.

Xiaoting Wang received the Ph.D. degree in physical geography from Institute of Mountain Hazards and Environment (IMHE), Chinese Academy of Sciences, Chengdu, China, in 2009. His research interest is urban sustainable development.

Ling Jiang (M'12) received the M.S. and Ph.D. degrees in geomatics from Wuhan University, Wuhan, China, in 2004 and 2008, respectively. Her research interest is urban remote sensing using very high resolution optical sensors.